DESIGN DATA SHEET
DEPARTMENT OF THE NAVY
NAVAL SEA SYSTEMS COMMAND

DDS 245-1

1 MARCH 1986

DDS 245-1 CONTROLLABLE PITCH PROPELLERS WITH BOLTED ON BLADES

CONTENTS

Paragraph	Title	Page
	Part I: INTRODUCTION	
245-1-a.	References	2
245-1-b.	Purpose and scope	4
245-1-c.	Approach	4
245-1-d.	Symbols and abbreviations	4
	Part II: GENERAL REQUIREMENTS	
245-1-e.	Specifications	4
245-1-f.	Stress calculations	5
245-1-g.	Fatigue analysis	5
	Part III: GUIDELINES AND PROCEDURES FOR BLADE ATTACHMENT DESIGN	
245-1-h.	Strength criteria	5
245-1-i.	Blade attachment design process	6
245-1-j.	Step one — examine dimensions and material properties	7
245-1-k.	Step two — apply simple load and stress prediction methods	7
245-1-l.	Step three — apply more accurate load and stress prediction methods	7

APPENDICES

	Appendix 1: METHODS OF PREDICTING BLADE LOADS	
A1-a.	Introduction	1-1
A1-b.	Centrifugal and gravitational loads	1-2
A1-c.	Hydrodynamic loads: steady-ahead in a calm sea	1-3
A1-d.	Hydrodynamic loads: maneuvers	1-6
A1-e.	Hydrodynamic loads: influence of rough seas	1-9
	Appendix 2: GUIDELINES FOR MINIMIZING BLADE LOADS	
A2-a.	Introduction	2-1
A2-b.	Stern Geometry	2-1

Paragraph	Title	Page
A2-c.	Preliminary propeller design	2-1
A2-d.	Detailed propeller blade design	2-2
A2-e.	Propulsion control system	2-2
A2-f.	Operating guidelines	2-3
Appendix 3:	COMPARISON METHOD FOR BLADE BOLTS AND CLOSED FORM STRESS ANALYSIS METHODS FOR BLADE BOLTS AND BLADE CARRIER	
A3-a.	Simple comparison method for blade bolts	3-1
A3-b.	Closed form stress analysis methods for blade bolts	3-2
A3-c.	Closed form stress analysis methods for blade carrier	3-5

TABLES

Table I:	Examples of Materials and Material Characteristics	8
II:	Dimensional and Nondimensional Comparison of Blade Attachments	9
1-I:	Summary of Design Tools and Estimated Accuracy For Predicting Propeller Blade Loads	1-4

FIGURES

Figure 1:	Dimensions Used in Table II for Hub and Blade Flange	10
2:	Dimensions Used in Table II for Blade Flange	11
3:	Dimensions Used in Table II for Crank Ring	12
4:	Dimensions Used in Table II for Blade Bolts	13
5:	Blade Load and Stress Variation with Time	14
1-1:	Components of Blade Loading	1-1
3-1:	Assumptions for Comparison Method for Blade Bolts	3-1
3-2:	Relationship Between Joint Force and Average Tension Bolt Stress	3-4
3-3:	Crank Ring Dimensions and Terminology	3-7

PART I. INTRODUCTION

245-1-a. References

(1) Boswell, R.J. et al., "Experimental Time Average and Unsteady Loads on the Blades of a CP Propeller Behind a Model of the DD-963 Class Destroyer," Propellers '78 Symposium, The Society of Naval Architects and Marine Engineers, Publication S-6 (1978).

(2) Kerwin, J.E. and C.S. Lee, "Prediction of Steady and Unsteady Marine Propeller Performance by Numerical Lifting Surface Theory," Transactions of the Society of Naval Architects and Marine Engineers, Vol. 86, pp. 218-253 (1978).

(3) Rubis, C.J. and T.R. Harper, "The Naval Gas Turbine Ship Propulsion Dynamics and Control Systems Research and Development Program," The Society of Naval Architects and Marine Engineers Paper No. 10 presented at Annual Meeting, New York, N.Y., (1982).

(4) Boswell, R.J. et al., "Experimental Determination of Mean and Unsteady Loads on a Model CP Propeller Blade for Various Simulated Modes of Ship Operation," The Eleventh Symposium on Naval Hydrodynamics, Sponsored Jointly by the Office of Naval Research and University College, London, Mechanical Engineering Publication Limited, London and New York, pp.789-823, 832-834 (Apr 1976).

(5) Jessup, S.D. and R.J. Boswell, "The Effects of Hull Pitching Motions and Waves on Periodic Propeller Blade Loads," Fourteenth Symposium on Naval Hydrodynamics, The University of Michigan, Ann Arbor, Michigan (1982).

(6) Boswell, R.J. et al., "Periodic Single-Blade Loads on Propellers in Tangential and Longitudinal Wakes," Propellers '81 Symposium, The Society of Naval Architects and Marine Engineers Publication S-7, pp. 181-202 (May 1981).

(7) Tasaki, R., "Propulsion Factors and Fluctuating Propeller Loads in Waves," Proceedings of the Fourteenth International Towing Tank Conference, Report of Seakeeping Committee, Appendix 7, Vol. 4, pp. 224-236 (1975).

(8) Oosterveld, M.W.C. (Editor), "Report of the Seakeeping Committee," Fifteenth International Towing Tank Conference, The Netherlands Ship Model Basin, Wageningen, The Netherlands, pp. 55-114 (1978).

(9) Day, W.G. et al., "Experimental and Prediction Techniques for Estimating Added Power Requirements in a Seaway," Proceedings of the Eighteenth American Towing Tank Conference, U.S. Naval Academy, Annapolis, MD, Vol. I, pp. 121-141 (1977).

(10) Lloyd, A.R.J.M. and R.N. Andrew, "Criteria of Ship Speed in Rough Weather," Proceedings of the Eighteenth American Towing Tank Conference, U.S. Naval Academy, Annapolis, MD, Vol. II, pp. 541-565 (1977).

(11) Lewis, E.V., "Motion of Ships in Waves," Chapter IX, Principles of Naval Architecture, Edited by J. P. Comstock, The Society of Naval Architects and Marine Engineers, pp. 607-717 (1967).

(12) Bjorheden, O., "Highly Skewed Controllable Pitch Propeller," 73rd Annual Meeting of the German Ship Technical Society, STG, Berlin, Germany (Nov 1978).

245-1-b. Purpose and scope

Design Data Sheet DDS 245-1 provides general guidelines for design and evaluation of the blade attachment mechanisms for Controllable Pitch (CP) propellers with bolted on blades. Classical methods of stress analysis are not generally applicable to blade attachment mechanisms due to their complex form and the high levels of alternating stresses. This DDS supplements Mil. Spec. DOD-P-24562.

Methods developed for prediction of blade loads are shown in Appendix 1. Appendix 2 provides guidelines for minimizing blade loads. Stress analysis methods are shown in Appendix 3.

245-1-c. Approach

The approach involves a three step evaluation process. This process is intended for use after the components of the blade attachment and hub have been sized, materials selected, and the supporting design calculations have all been completed. The steps are: (1) Examine Dimensions and Material Properties, (2) Apply Simple Load and Stress Prediction Methods, (3) Apply More Accurate Load and Stress Prediction Methods.

The appendices provide methods for predicting blade loads and guidelines to reduce those loads, along with methods for the stress analysis in the critical areas of the blade bolts and blade carrier. These methods may help in steps Two and Three of the evaluation process.

In design and analysis, measurements and properties may be expressed in either inch-pound or SI(metric) units, unless a specific unit system is specified in the ordering document.

245-1-d. Symbols and abbreviations

The symbols and abbreviations are described within the text, tables, and figures.

Part II. GENERAL REQUIREMENTS

245-1-e. Specifications

The basic ordering document for CP propellers is Mil. Spec. DOD-P-24562. Some criteria included in this specification are:

1. Charpy impact strength requirements for propeller blade attachment components.
2. Minimum fatigue life requirements for propeller blade attachments.
3. Torque requirements for propeller blade bolts.

245-1-f. Stress calculations

Calculations of stresses in hub components cannot ignore the effects of deformations of the hub casting and blade attachment components, as this results in calculated stresses which are considerably lower than actual stresses. A more sophisticated analysis is necessary. Accurate knowledge of propeller blade attachment component stresses is required because these stresses affect the hub diameter which, in turn, affects propeller efficiency.

The distribution of stresses among the blade bolts and, therefore, the maximum blade bolt stress, depend upon the "stacking" (blade rake and blade skew) of the blade sections relative to the spindle axis. Significant stress reduction can be obtained by changes in stacking. Closed form stress analysis methods for blade bolts and blade carriers are provided in Appendix 3.

245-1-g. Fatigue analysis

To calculate the fatigue life of propeller hub components, the following must be known:

1. Fatigue life curves for the materials used. The safety factor to be applied to the curves. Reduction in the safety factor is possible where fatigue tests of the actual component have been conducted.
2. Time-average stresses on the propeller blades.
3. Alternating stresses on the propeller blades. Methods for calculating alternating propeller blade forces are described in Appendix 1.
4. The relationship between alternating stress, shaft r/min, and rudder angle in each operating mode.

Part III. GUIDELINES AND PROCEDURES FOR BLADE ATTACHMENT DESIGN

245-1-h. Strength criteria

Two stress criteria must be satisfied in order for the bolts and blade carrier to be considered adequate. The maximum stress must be less than the material's yield stress (except at the thread roots and bearing stress under the bolt head) and the spectrum of fatigue stresses must be within the material's endurance capacity.

The accuracy of the predicted stresses depends not only upon the accuracy of the stress analysis, but also upon the accuracy of the blade loads used in the analysis. Mean load at the steady-ahead, zero-rudder condition can be predicted to within 5 percent of the true value. On the other hand, predictions of unsteady or periodic loads during a sharp turn in rough seas may be in error by as much as 75 percent of the true value. Combined errors in the prediction of the maximum load in a turn might lead to its underprediction or overprediction by as much as 60 percent. In addition to the inaccuracies in

load predictions, there is always a significant degree of scatter in material properties, particularly those related to fatigue, which must be considered.

The choice of the margins of safety to apply to the predicted stresses depends upon the ship application and the confidence in the analyses used. It is desirable that the diameter and weight of the hub be as small as possible. However, it is essential that failures of hub components do not occur.

The following strength criteria are established as a baseline for use during initial design of blade attachments or for use with the "simple" load and stress prediction methods defined in para. 245-1-k. Because of error margins, these criteria are intentionally conservative as are the simple stress methods; when any one of the criteria is exceeded, additional evaluation of the blade attachment strength is required:

1. Maximum bolt shank stress including prestress is to be less than two-thirds of the bolt material yield stress;
2. Maximum blade carrier stress is to be less than one-half of the blade carrier material yield stress;
3. Maximum average bearing stress under the bolt heads is to be less than 90 percent of the yield stress of any affected material; and
4. Maximum fatigue stresses in the bolts and the blade carrier are to be less than 40 percent of the materials' endurance stress.

245-1-i. Blade attachment design process

The above considerations related to strength criteria and the increasingly sophisticated and costly array of methods for predicting both blade loads and resulting stresses have made it necessary to formalize the structural design process for CP propeller blade attachments. The complexity of the design process depends upon the magnitude of estimated stresses versus strength criteria at each of several possible decision points. Where all stresses are well below the previously noted criteria, factors of safety are inherently large and, therefore, only the more simple prediction methods for both loads and stresses will normally be appropriate. Where stresses exceed those criteria, the use of more accurate load and stress prediction techniques will be required, possibly along with experimental verification of computed stresses and suitable fatigue tests. It will also be reasonable to consider during the structural design process the possibility of decreasing stress levels through design modifications such as changes in blade fillet shape or increased radii at stress concentrations. Alternatively, strength problems might be alleviated by changes in materials or manufacturing methods such as rolling of bolt threads. The blade designs (not the blade attachment and hub) of U.S. Navy propellers are normally specified and will meet requirements for ship powering, vibration, cavitation, etc. In the design of CP propellers, balanced skew and forward rake of the blade will cause the blade mass center of gravity to be near or on the blade spindle axis which provides more uniform bolt loading due to centrifugal force. Further, it is possible to design blade fillet shapes which will lead to a more even distribution of bolt forces.

The following process shall be undertaken after the components of the blade attachment and hub have been sized, materials selected, and the supporting design calculations have all been completed.

245-1-j. Step one -- examine dimensions and material properties

1. Review the materials and material characteristics (such as yield, ultimate, and fatigue strengths, and toughness). Some examples of materials that have been used in recent U.S. Navy CP propellers are listed in Table I. Relate materials to such variables as availability, machinability, compatibility, reliability. List and calculate the data shown in Tables II(A) and II(B) and compare with previous experience. Deviations may indicate where the designer is depart ing from past practice and thus may indicate potential design problem areas.

2. Perform the Simple Comparison Method for Blade Bolts, described in Appendix 3. This method provides a preliminary overview and indication of bolt force level through comparisons with similar calculations for a number of successful and unsuccessful designs. Results from this analysis indicate whether bolts are relatively highly loaded (requiring closer examination) or lightly loaded.

245-1-k. Step two -- apply simple load and stress prediction methods

1. Perform the closed-form stress analysis methods for blade bolts and blade carriers, described in Appendix 3.

2. Compare the stresses obtained with the strength criteria in para. 245-1-h.

3. Blade loads and subsequent stresses vary as indicated in Figure 5, whether the ship is operating at zero rudder in a calm sea or at full rudder in rough seas. In many cases a model wake survey and calculation of the time-average and periodic loads under full-power steady-ahead operation in calm water are conducted as part of the design of the propeller blades. For these cases, use the time-average or mean loads and periodic loads at zero rudder that are provided. If no wake survey or prediction of loads is available, estimate the time-average and periodic loads under steady-ahead operation in calm water using the guidelines in Appendix 1.

The peak blade loads (the maximum blade loads considering the time-average, transient, and periodic contributions) generally occur during full-power, full-rudder turns in a calm sea or during high speed operation in rough seas, depending upon the operating characteristics of the ship. Estimate the peak and periodic blade loads by the use of the guidelines provided in Appendix 1.

4. Compare the predicted maximum and fatigue stresses obtained with the criteria in para. 245-1-h. If the criteria are satisfied, and the design is not very different from the designs on which these analyses are based as indicated by step one, para. 245-1-j, then the blade and blade carrier are capable of providing adequate structural performance. If the criteria are not satisfied, continue on to step three.

245-1-l. Step three -- apply more accurate loan and stress prediction methods

Note: Unless otherwise directed, this step may be eliminated under the following circumstances:

a. The hub design is similar to previous successful designs by the same manufacturer, and

b. The criteria stated in para. 245-1-k are met or exceeded.

	Example A	Example B	Example C
Crank Ring			
Material	Steel A471-70, Cl 6	Steel HY-100	Steel A243-64, cl J
Yield Stress (ksi)	130(min)	100	60(min)
Ultimate Strength (ksi)	140(min)	-	90(min)
Fatigue Strength (ksi)	55	50	-
Toughness (minimum Charpy-V, ft-lb)	40(RT)	30(120 deg F)	-
Blade Bolts			
Material	K-Monel	Steel 17-4PH	-
Yield Stress (ksi)	100	100	-
Ultimate Strength (ksi)	160	135	-
Fatigue Strength (ksi)	40	65	-
Toughness (minimum Charpy-V, ft-lb)	21	20	-

Table I: Examples of Materials and Material Characteristics

(A)

DIMENSIONAL COMPARISON
MATERIALS
Blade
Blade Bolts
Blade Carries
Hub
GENERAL DESCRIPTION
Hub type (Figure 1)
Blade Carrier type
Number of bolts
Number of blades
Method of bolt preloading
Cover plate
DIMENSIONS
Blade tip radius, r_{blade}
Hub (Figure 1)
Radius, r_{hub}
Radius forward, r_{hf}
Radius aft, r_{ha}
Blade Flange or Palm (Figures 1 and 2)
Radius, r_{flg}
Radius of bolt circle, r_{BC}
Radius of counterbore, r_{CB}
Radius of through bolt hole, r_b
Radius of dowel pin, r_{dp}
Thickness of counterbore, t_{cb}
Distance to inner flange surface, d_{fl}
Crank Ring (Figure 3)
Outer radius, R_o
Inner radius, R_i
Fillet radius, r_f
Thickness of wall, t_{wall}
Thickness of lip, t
Maximum thickness, t_{max}
Distance to top bolt thread, x_t
Distance to bottom bolt thread, x_b
Blade Bolts (Figure 4)
Bolt head radius, r_{bh}
Bolt shank radius, r_{bs}
Bolt thread radius, r_{bt}
Length of threads, l_{bt}
Length of shank, l_{bs}

(B)

NONDIMENSIONAL COMPARISON
Hub (Figure 1)
r_{hub}/r_{blade}
r_{hf}/r_{blade}
r_{ha}/r_{blade}
Blade Flange or Palm (Figure 1 or 2)
r_{flg}/r_{hub}
r_{BC}/r_{flg}
r_b/r_{BC}
r_{CB}/r_{BC}
t_{cb}/r_b
r_{dp}/r_{BC}
d_{fl}/r_{hub}
Crank Ring (Figure 3)
R_o/r_{hub}
R_i/R_o
r_{BC}/R_o
t_{wall}/r_{bt}
x_t/x_b
r_f/R_i
t/t_{max}
t_{max}/r_{hub}
Blade Bolts (Figure 4)
r_{bh}/r_{BC}
r_{bs}/r_{BC}
r_{bt}/r_{BC}
$(l_{bt} + l_{bs})/r_{bs}$

Table II: Dimensional and Nondimensional Comparison of Blade Attachments

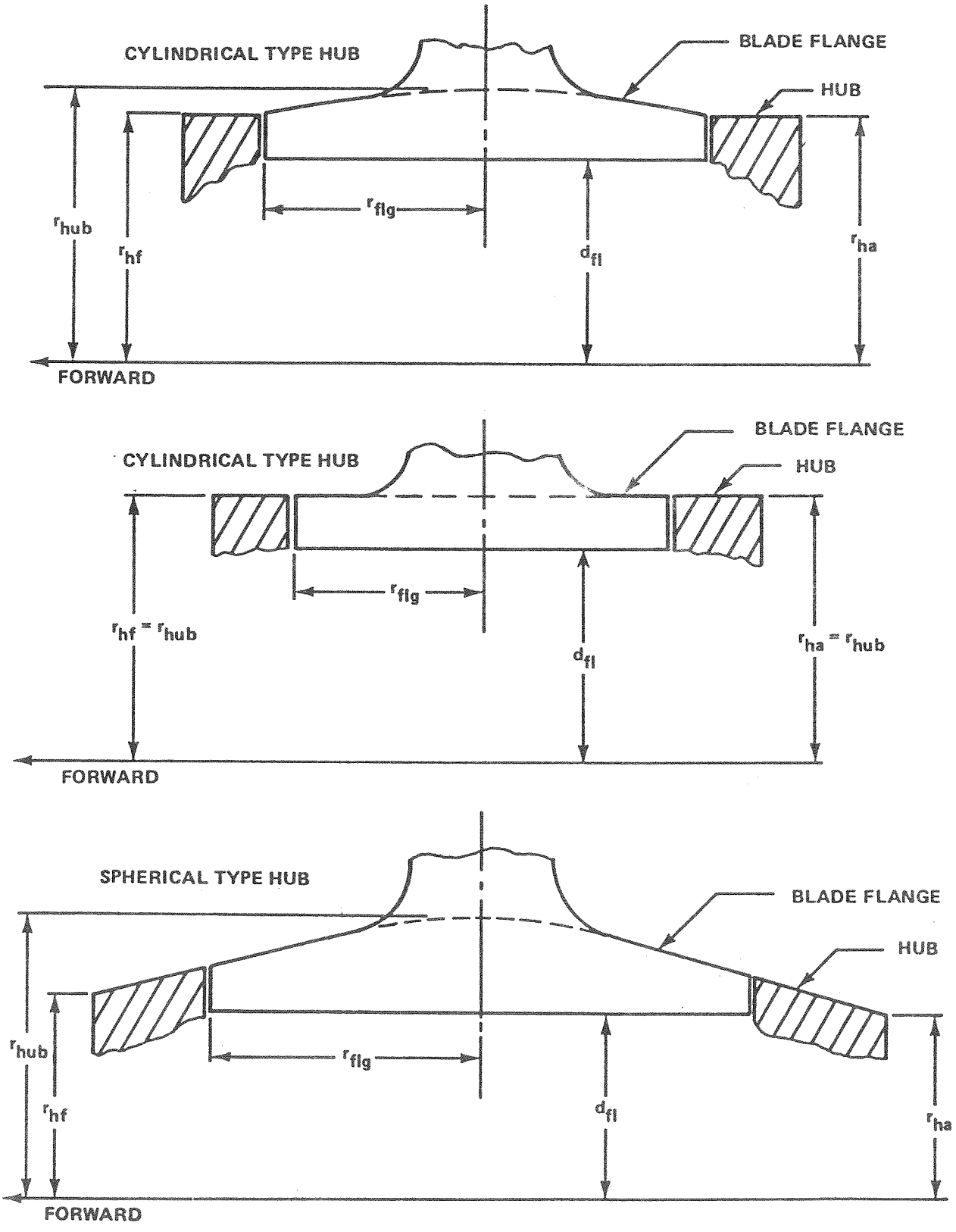

Figure 1 - Dimensions Used in Table II for Hub and Blade Flange

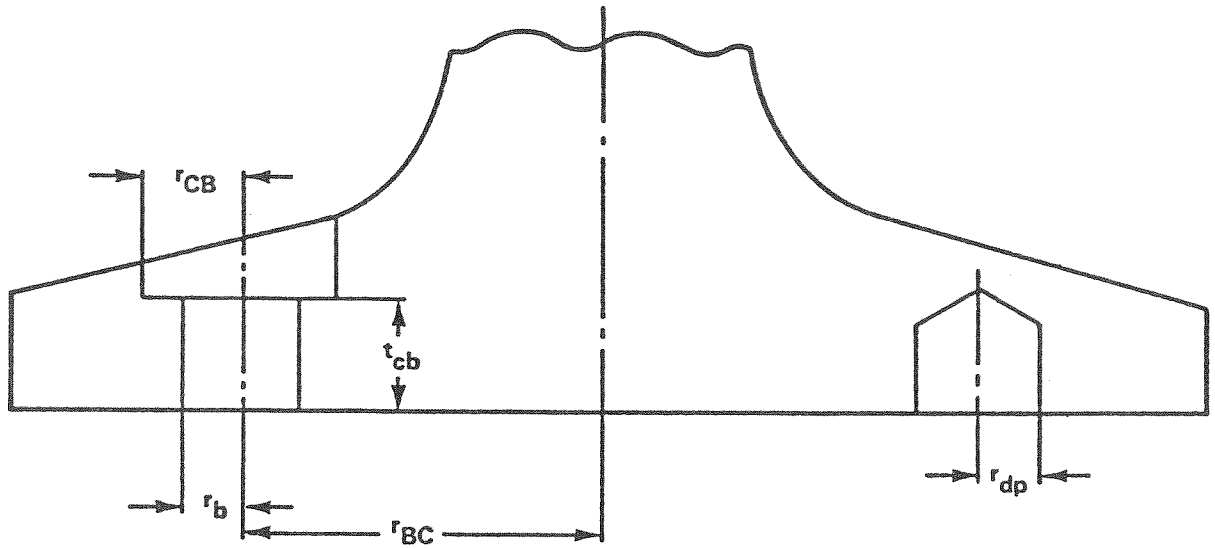

Figure 2 - Dimensions Used in Table II for Blade Flange

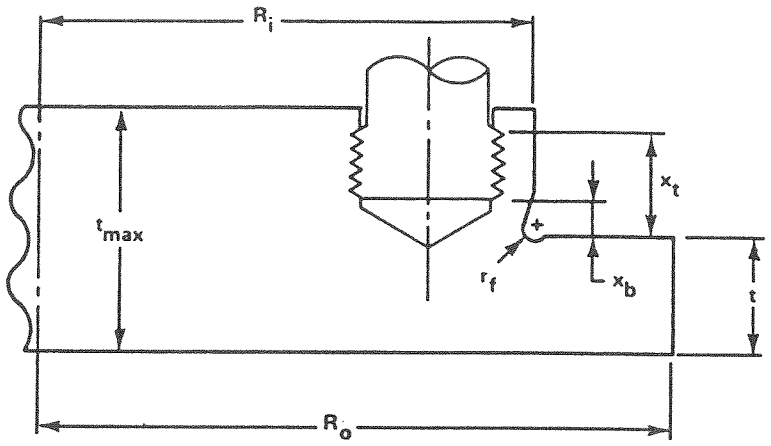

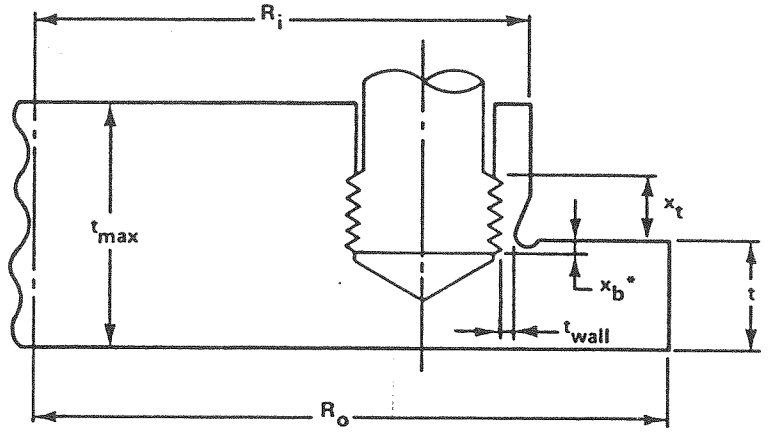

*NOTE: x_b AND x_t ARE NEGATIVE WHEN BOLT THREADS ARE DEEPER IN CRANK RING THAN FLANGE SURFACE.

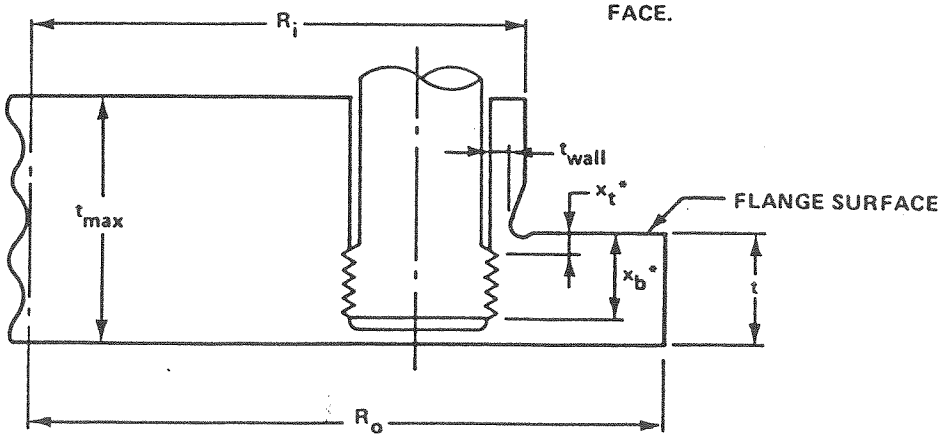

Figure 3 - Dimensions Used in Table II for Crank Ring

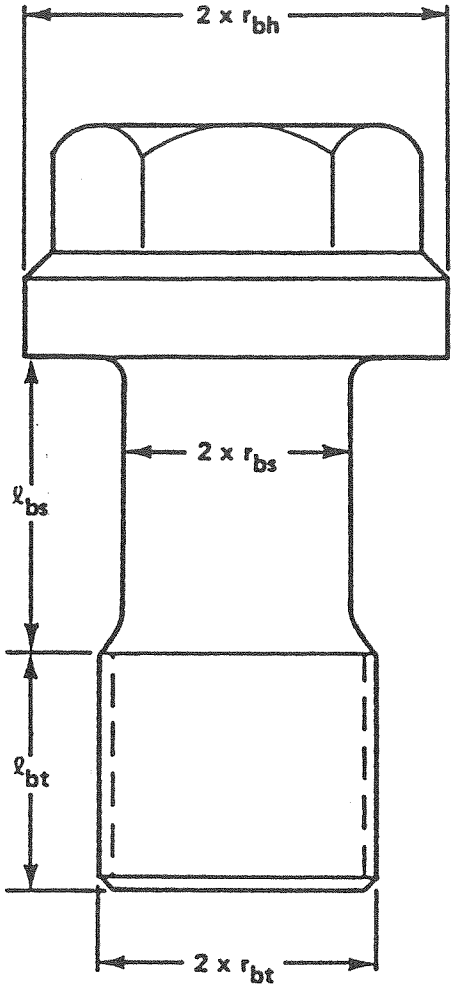

Figure 4 - Dimensions Used in Table II for Blade Bolts

1. To obtain more accurate predictions of periodic blade loads under steady-ahead operation in a calm sea: Measure loads on a scale model using the procedures described in Appendix 1. Cross-check these measurements with theoretically calculated periodic blade loads based on the wake measured in the plane of the propeller behind the model hull.

2. To obtain more accurate predictions of the peak and periodic blade loads during high speed turns in a calm sea: Conduct model wake surveys in simulated turns. Calculate the periodic and peak loads based on these wake surveys using methods described in Appendix 1.

3. To obtain more accurate predictions of the increase in peak, transient, and periodic blade loads due to the influence of a rough sea: Measure loads on a scale model using the procedures described in Appendix 1.

4. To obtain more accurate predictions of stresses: Conduct a full three-dimensional finite element (FE) analysis of the blade, bolts, blade carrier, and portions of the hub. This method can be combined with two-dimensional FE methods to examine stresses in areas such as the crank ring fillet or the bolt head to shank fillet. The three-dimensional method also provides a prediction of the amount of bolt bending which is not possible with the simpler methods. The simpler methods use an empirical factor of 2.0 to account for bolt bending. A structural model experiment may also be used.

5. Special examinations may be necessary in certain areas. For example, it may be claimed that a particular type of bolt has fatigue properties which exceed those obtained by Equations (7) and (8) in Appendix 3. These claims would require corroboration with fatigue test data on actual hardware.

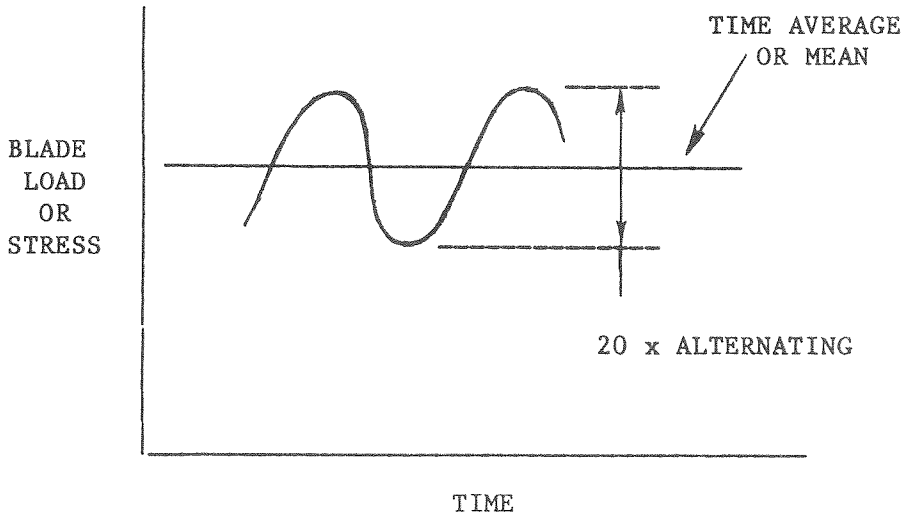

Figure 5 - Blade Load and Stress Variation with Time

APPENDIX 1

METHODS OF PREDICTING BLADE LOADS

A1-a. Introduction

This appendix describes the available techniques for predicting blade loads under various operating conditions.

The blade loading transmitted to the hub can be represented as three force components and three moment components along a set of orthogonal axes. The coordinate systems shown in Figure 1.1 are used in the present calculation.

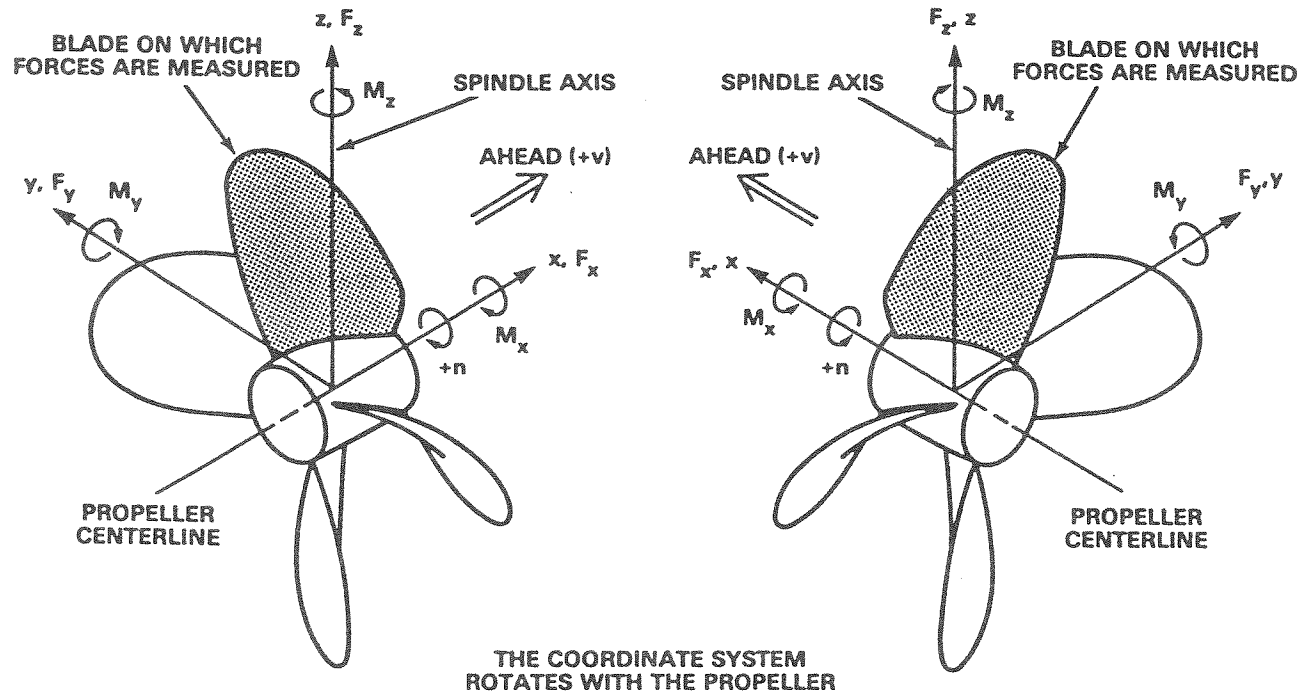

Figure 1.1 - Components of Blade Loading

The F_X, M_X, F_y, and M_y components (see Figure 1.1) can also be resolved into the magnitude and direction of a force and bending moment about some reference radius such as the radius of the bolting face of the blade carrier. For hydrodynamic loads, the directions of these force and moment vectors are, approximately, perpendicular and parallel, respectively, to the blade pitch line at the 70 percent radius for all operating conditions except crashback maneuvers. The spindle torque M_Z is, in general, substantially less than the bending moments M_X and M_y. Spindle torque M_Z is important from considerations of

controlling the blade pitch, and may, depending upon the blade skew, significantly contribute to high stresses in various components of the hub mechanism. The role of skew in minimizing M_z is discussed in Appendix 2 on Guidelines for Minimizing Blade Loads.

A1-b. Centrifugal and gravitational loads

The centrifugal loading, which is a function only of the blade geometry, blade density, and propeller rotational speed, has only time average and transient components.

Centrifugal loading can be represented as a concentrated radial force through the blade centroid, and transmits primarily an $F_{z,c}$[+] component to the hub; see Figure 1.1. However, depending upon the blade rake and skew, centrifugal loads can also produce substantial bending moment components $M_{y,c}$ and $M_{x,c}$ The propeller blade designer has essentially no control over the value of $F_{z,c}$ after the preliminary design stage in which propeller diameter and rpm are fixed; however, the designer can control $M_{y,c}$, and to a lesser extent $M_{x,c}$, by the proper selection of blade rake and skew. It is desirable to minimize the total (hydrodynamic plus centrifugal) values of loading components, and the hydrodynamic portion $M_{y,H}$[+] is inherently positive (see Figure 1.1 for sign convention) and is the largest moment component for all operating conditions except deceleration and backing. Therefore, it is desirable to have $M_{y,c}$ negative, which can be achieved by placing the blade centroid forward of the spindle axis. This requires negative rake[++] or skew[+++].

Requirements to minimize propeller-induced vibratory forces and spindle torque under steady-ahead operation dictate a balanced skew with negative skew at the inner radii and positive skew at the outer radii. This inherently places the blade centroid near the spindle axis for an unraked blade so that $M_{y,c}$ and $M_{x,c}$ are small. Blade rake has no influence on $M_{x,c}$, but $M_{y,c}$ varies directly with rake when all other parameters are held constant. Therefore, it is desirable to apply as much negative rake as practical from considerations of clearances, design theory, and total blade geometry. In summary, balanced skew and negative rake are recommended from considerations of centrifugal blade loads.

Gravitational loading is a function only of the blade geometry and blade density and occurs primarily as a first harmonic of blade angular position.

The gravitational loads can be represented as a constant downward force (the weight of the blade in water) applied at the centroid of the blade. The magnitude and centroid of blade weight are generally calculated during the propeller design process. The blade weight is generally an order of magnitude less than the time-average thrust under full-power steady-ahead operation. The blade weight has a constant F_x component, $F_{x,g}$,* and a first harmonic component of F_y, F_z, M_x, M_y, and M_z relative to a coordinate system rotating with the propeller blade. Force component $\bar{F}_{x,g}$** is negligible relative to $\bar{F}_{x,H}$ for realistic shaft inclination angles. The amplitudes of $(M_y)_{1,g}$*** and $(M_z)_{1,g}$, which are essentially the product of the weight of the blade and the x

---

NOTE:

+ The subscript c denotes centrifugal loads; H denotes hydrodynamic loads.
++ Rake is positive aft.
+++Skew is positive aft (towards trailing edge).
* The subscript g denotes gravitational loads.
** The superscript $\bar{}$ denotes time-average loads.
***The notation $(\ )_1$ denotes the first harmonic of ( ).

coordinate of the blade centroid relative to the spindle axis, are negligible relative to the respective hydrodynamic components. The amplitude of $(F_z)_{1,g}$ is essentially the weight of the blade which is, in general, less than three percent of $\bar{F}_z$ which is essentially the centrifugal force on the blade. Therefore, $(F_z)_{1,g}$ can be neglected. Components $(F_y)_{1,g}$ and $(M_x)_{1,g}$ are, in general approximately 180 degrees out of phase with and smaller than the respective components of hydrodynamic loading for wakes behind high-speed transom sterns with exposed struts and shafting, that is, for wakes of the type encountered on surface combatants. Therefore, the neglect of these components results in a slightly conservative prediction of the maximum periodic blade bending moment. In summary, the gravitational loads may be completely neglected without a significant loss in accuracy of the predicted total loads.

A1-c. Hydrodynamic loads: steady-ahead in a calm sea

This and the following two paragraphs discuss the use of available techniques for determining hydrodynamic loads and their associated inaccuracies as they are applicable to CP propeller design. The available techniques have been discussed in paras. 245-1-k and 245-1-l. The estimated inaccuracies or errors are summarized in Table 1-I.

The blade loading transmitted to the palm is represented as the three force components and three moment components shown in Figure 1-1. For the radial force component F_z, the hydrodynamic loads are relatively unimportant because essentially all of the time average and transient portions of F_z arise from centrifugal force, and most of the periodic portion of F_z, which is quite small, arises from gravitational loads.

Time-average loads. Time-average loads under steady-ahead operation in a calm sea may be predicted by any one of several methods:

1. Routine model powering experiments. Routine model powering experiments yield predictions of time-average thrust and torque over the speed range. Blade bending moments about any desired radius equal to or less than the radius of the blade palm can be calculated from these measured quantities by assuming a radial point of application of thrust $\bar{F}_x$ and transverse force $\bar{F}_y$. An estimat of the radial points of application of these force components can be obtained from propeller design or analysis calculations; if these are unavailable, assum that these force components are applied at the 0.7 radius. The true radial centers of these force components are generally within 2 percent of the 0.7R; therefore, errors resulting from assuming that these radial centers are located at 0.7R can result in an error of ± 5 percent in the moment arms at the blade carrier (at approximately 0.25R). These experiments predict thrust and torque to within approximately ± 3 percent, and blade bending moments at the blade carrier to within approximately ± 8 percent. These experiments yield no information on spindle torque M_z.

2. Propeller design calculations. The distribution of hydrodynamic loads over the blade at the design condition* is determined during the process of designing the propeller blades. This yields the F_x, F_y, M_x, and M_y

---

NOTE:

* The design condition is defined as the steady-ahead condition in calm water at which the detailed design of the propeller blades is conducted. This condition generally corresponds to a specified speed or delivered power, and a specified propeller rotational speed.

Table 1-I: Summary of Design Tools and Estimated Accuracy For Predicting Propeller Blade Loads

	Time-Average and Transient Loads	Error[1] ± Percent	Periodic Loads[2]	Error[1] ± Percent
Steady-ahead in a calm sea	Design calculations	5	Model blade loading experiments	15
	Model powering experiments	8	Theory plus empirical factor	20
	Theory	10	Statistical data	30
Acceleration and deceleration in a calm sea	Computer simulation[3]	15	Theory plus empirical factor	25
	Statistical data	40	Statistical data	40
Turning maneuvers in a calm sea	Computer simulation[3]	20	Theory plus empirical factor with model wake survey in turn	30
			with estimated wake in turn	40
	Statistical data	40	Statistical data with model wake survey in turn	45
			with estimated wake in turn	60
Steady-ahead in rough water	Model experiments in rough water[4]	15	Semi-empirical theory[3,6]	30
	Statistical data[4]	25		
	Semi-empirical theory[3,5]	20		

All errors are ± "true" value in percent.

[1]Errors shown apply to the F_x, M_y, F_y, and M_x component, the deviations from "true" values for M_z are approximately twice the values shown.

[2]Assumes that the most accurate method listed was used to predict time-average or transient loads.

[3]Requires same supporting model experiments.

[4]Time-average values.

[5]Transient values.

[6]Assumes that the most accurate method listed was used to predict periodic loads in calm sea.

components within approximately ± 5 percent of their true values and the M_z component within approximately ± 10 percent of its true value. The predicted spacial distributions of loading are applicable only at the design advance coefficient J; however, the radial distributions of these loads are insensitive to J over the range of J encountered by a surface combatant under steady-ahead operation in a calm sea. Therefore, the blade bending moments over the speed range may be calculated using the radial centers of thrust and transverse force from the design calculations, and the thrust and torque as a function of speed from routine model powering experiments.

3. Propeller inverse theory. The distribution of time-average hydrodynamic loads over a propeller blade can be calculated by propeller lifting-surface theory (Reference 1) given propeller geometry, radial distribution of inflow, and operating conditions. This yields the F_x, F_y, M_x, and M_y components within approximately ± 10 percent and the M_z component within approximately ± 20 percent. The primary use of this method is for applications in which the design calculations are unavailable or unsuitable, such as off-design conditions. The predicted radial centers of F_x and F_y from this method can also be used with the thrust and torque predicted from routine powering experiments to more accurately calculate the blade bending moments.

Periodic loads. Periodic blade loads under steady-ahead operation in a calm sea shall be predicted by the following methods:

1. Model experiments. Measure the six components of blade loading on a model of the propeller-hull configuration. This yields the periodic portions of F_x, F_y, M_x, and M_y components within approximately ± 15 percent of their true values, and the periodic portion of M_z within approximately ± 30 percent of its true value.

2. Analytical calculations. Calculate periodic blade loads using unsteady lifting surface theory with an empirical factor of 1.4 derived from extensive correlations between this method and experimental data (see References 1,2,5 and 6). A wake survey conducted behind the model hull is a necessary input to this calculation. This method yields $\tilde{F}_x$, $\tilde{F}_y$, $\tilde{M}_x$, and $\tilde{M}_y$* within approximately ± 20 percent of their true values, and $\tilde{M}_z$ within approximately ± 40 percent of its true value.

3. Statistical data. Estimate periodic blade loads directly from the existing statistical data base of model and full-scale measurements of periodic blade loads. The accuracy of estimates using this procedure depends upon the degree of similarity between the new configuration including propeller geometry wake, and operating conditions and the configurations in the database, and upon the physical insight of the person making the estimates. For a new configuration which is somewhat similar to the configurations in the database, a person with reasonable insight could probably estimate F_x, F_y, M_x, and M_y within approximately ± 30 percent of their true values, and M_z within ± 60 percent of its true value.

> NOTE: For a propeller-hull configuration which is similar to an existing configuration, the model experiment measurements may be omitted.

NOTE:

* The superscript $\sim$ denotes the periodic portion of loads.

A1-d. Hydrodynamic loads: maneuvers

Transient loads.

1. Computer dynamic simulation. Transient loads during maneuvers, including acceleration, deceleration, and various types of turning maneuvers, depend upon the instantaneous values of ship speed, propeller rotational speed, propeller pitch, and propeller-hull interaction coefficients. The transient loads, or time-average loads per revolution, appear to be insensitive to the time rate of change of the aforementioned variables. Therefore, if the time histories of these variables through a maneuver are known, the time-average loads may be estimated from routine propeller model thrust and torque characteristics in uniform flow (propeller open water characteristics) and propeller inverse lifting-surface theory (Reference 2) as described in Paragraph A1-c on steady-ahead operation.

The time histories of ship speed, propeller rotational speed, propeller pitch, and propeller-hull interaction coefficients during a specific maneuver depend, in a complex manner, upon interactions between the characteristics of the propeller, hull, prime mover, and control system. For a new ship design the best method of predicting the time histories of the aforementioned variables is a computer dynamic simulation of the complete propulsion system and ship response, such as that described in Reference 3. These dynamic simulations require accurate knowledge of the individual characteristics of the propeller, hull, propeller-hull interaction, prime mover, and control system.

The individual characteristics of the propeller, hull, and propeller-hull interactions over the pertinent range of conditions likely to be encountered during maneuvers must be obtained from systematic model experiments on the propeller and hull under consideration. These experiments include open-water characterization of the propeller and associated blade spindle torque measurements over a range of conditions including ahead and astern velocities, each over a range of positive and negative pitches, determination of the pertinent maneuvering coefficients of the hull, and determination of the propeller-hull interaction coefficients over the pertinent range of conditions.

The accurate determination of the propeller-hull interaction coefficients is the most difficult and weakest part of the simulation. There exist very few reliable measurements of these interaction coefficients under conditions likely to be encountered during maneuvers. Interaction coefficients are difficult to determine accurately and are very sensitive to small changes in many parameters. It is difficult to interpolate or extrapolate them without further loss of accuracy. This is particularly true for turning maneuvers. In addition to those listed previously, parameters in turns include roll, drift angle, rudder angle, unbalances between the propellers on twin-screw ships, and interactions between the various parameters.

In simulating turning maneuvers, the path and orientation of the hull have a significant influence on the loads. These can be predicted with four-degrees-of-freedom maneuvering simulation programs which use the pertinent maneuvering coefficients of the hull as determined from model experiments. Usually, four-degrees-of-freedom programs predict ship motion characteristics without regard for propeller thrust and torque, but they can be modified to include propeller thrust and torque as a function of propeller rotational speed ship velocity, and ship orientation (Reference 3). With this refinement, the influence of the path and orientation of the hull can be incorporated into the dynamic simulation.

Computer dynamic simulations, supported by model experiments on the propeller and hull, yield predictions of the maximum transient values of the F_x, F_y, M_x, and M_y components of blade loading within approximately ± 15 percent for acceleration and deceleration maneuvers, and within approximately ± 20 percent for turning maneuvers. The deviations from the true values for M_z are approximately twice the percentages for the other components. If the computer dynamic simulations use propeller, hull, or propeller-hull interaction coefficients approximated from hulls or propellers that are different from the final configuration, then the inaccuracies in predicting the blade loads become somewhat greater.

2. Statistical data. Transient blade loads can be estimated from the statistical database of full-scale measurements and computer dynamic simulations on previous ships. The method is less accurate than the use of computer dynamic simulations supported by model experiments. The accuracy of estimates using this procedure depends upon the degree of similarity between the new configuration and the configurations in the database, including propulsion control system, stern geometry, propeller geometry, and types of maneuvers, and upon the physical insight of the person making the estimates. For a configuration which is similar to configurations in the database, a person with reasonable insight could probably estimate the maximum values of F_x, F_y, M_x, and M_y within approximately ± 40 percent of their true values, and the maximum value of M_z within ± 100 percent of its true value for acceleration, deceleration, and turning maneuvers. For a configuration which is significantly different from an existing configuration, the inaccuracies become somewhat greater.

Periodic Loads.

1. Analytical calculations. The periodic loads during maneuvers, including acceleration, deceleration, and various types of turning maneuvers, depend upon the same parameters as discussed in the preceding paragraphs for transient loads, except that the dependence upon the propeller-hull interaction coefficients may not be as strong. However, unlike the transient loads, the periodic loads depend critically upon the spacial distribution of the wake velocity components in the propeller at a given time in a maneuver. Therefore, two basic inputs are required for predicting periodic blade loads in a maneuver:

(a) A time-history of the maneuver, that may be estimated using computer dynamic simulations and/or the statistical database of full-scale measurements (as described above under Transient Loads), and

(b) An estimate of the wake velocity components in the propeller plane at a given time in the maneuver.

For acceleration and deceleration maneuvers, the nondimensional wake velocity components for ahead speed ($V > 0$) are approximately the same as for stead-ahead operation. For astern speed ($V < 0$), the periodic loads are, in general, small due to the relatively low magnitudes of V and rotational speed n under these conditions, so that it is not usually necessary to estimate accurately the wake velocity components. If desirable, model wake surveys can be conducted under astern operation simulated in a quasi-steady manner, that is, $V < 0$, $\dot{V} = 0$.*

The circumferential variations of the wake velocity components in the propeller become more severe in turning maneuvers than for steady-ahead operation due to the large drift angle, that is, the angle between the local

---

NOTE:

* A superscript $\cdot$ means $\frac{d}{dt}$.

undistributed direction of motion and the hull centerline. This drift angle is in principle equivalent to the inclination angle of the flow relative to the propeller shaft for steady-ahead operation, except that it occurs in the horizontal plane. Therefore, this drift angle produces a large first harmonic tangential wake, and thereby produces large first harmonic periodic loads.

Wake surveys conducted on models of high-speed transom stern configurations during simulated steady turns show that the circumferential variation of the wake is dominated by the drift angle at the propeller plane. The peak to peak circumferential variation of the velocity components of the wake of a high-speed transom stern configuration with exposed shafting and struts in a turning maneuver can be estimated within approximately ± 20 percent from the known wake velocity components under steady-ahead operation, the drift angle at the propeller plane, and the location of the propeller in the turn, that is, inboard, outboard, or centerline.

A more accurate estimate of the wake velocity components can be obtained from a model wake survey conducted on a model of the hull at the conditions existing at a given time in the maneuver simulated in a quasi-steady manner, that is, constant values of ship speed, drift angle, turning radius, roll, etc. This model wake survey should be run for conditions at which nearly maximum values of periodic loads are predicted.

Once the time-history of the maneuver including the wake velocity components is estimated, the periodic loads at any time during the maneuver can be calculated using the same procedures as for steady-ahead operation. For preliminary estimates to determine at what conditions the largest peak and periodic loads occur, the periodic loads can be estimated from the calculated or measured periodic loads under steady-ahead operation, adjusted for operating conditions and wake patterns using trends of previous data as a guide; see References (1) and (4) through (6) for examples of data.

If the time-history of the maneuver is predicted by the best available methods, then the maximum values of the $\tilde{F}_x$, $\tilde{F}_y$, $\tilde{M}_x$, and $\tilde{M}_y$ components during acceleration and deceleration maneuvers can be predicted by analytical calculations plus an empirical factor of 1.4 within approximately ± 25 percent. Similarly, the maximum values of the $\tilde{F}_x$, $\tilde{F}_y$, $\tilde{M}_x$, and $\tilde{M}_y$ components during turning maneuvers can be calculated within approximately ± 30 percent if model wake surveys during simulated turns are conducted, and within approximately ± 40 percent if the wake patterns during the turns are approximated from the drift angle and the wake data during steady-ahead operation or the statistical wake data in the literature. The deviations from the true values for the M_z component are approximately twice the percentages for the other components.

2. Statistical data. The periodic blade loads on a propeller-hull configuration can be estimated from the statistical database of model and full-scale measurements and analytical calculations of periodic blade loads. This method is less accurate than the analytical calculation method. The accuracy depends upon the degree of similarity between the new configuration and the configurations in the database, including propeller geometry, wake, and operating conditions, and upon the physical insight of the person making the estimates. If the time-history of the maneuver is predicted by the best available methods, then, for a configuration similar to the configurations in the database a person with reasonable insight could probably estimate the maximum values of F_x, F_y, M_x, and M_y within ± 40 percent of their true values for acceleration and deceleration maneuvers, within ± 45 percent for turning maneuvers using measured wakes on the configuration in simulated turns, and within ± 60 percent for turning maneuvers using estimated wakes in turns. The

deviations from the true values for the M_z component are approximately twice the percentages for the other components.

A1-e. Hydrodynamic loads: influence of rough seas

When a ship operates in rough seas, the ship speed and propeller rotational speed at a given delivered power decrease from the corresponding values in calm water due to increased resistance of the hull and change in the propulsion coefficients (involuntary speed loss)(References 7-9). Furthermore, in rough seas the delivered power is often reduced from the calm water value (voluntary speed loss)(References 8, 10). Therefore, the difference in blade loads between operation in calm seas and operation in rough seas can be represented as being made up of two major parts:

1. Differences in loads resulting from the difference in ship speed and propeller rotational speed between calm seas and rough seas, and
2. Increases in loads due to the direct influence of waves and ship motions at a given value of ship speed and propeller rotational speed.

Time-average loads. The changes in the time-average* propeller rotational speed, speed of advance, thrust, and torque at a given delivered power due to operation in rough seas can be estimated experimentally or theoretically. Examples of methods or data are summarized by Oosterveld, (Reference 8) Day et al., (Reference 9) and Lloyd and Andrew. (Reference 10) The most accurate approach is to conduct model experiments using the experimental procedures summarized by Day et al. (Reference 9)

For a given operating condition and time-average thrust and torque, the time-average values of the various components of blade loading can be calculated using the pertinent procedures as described in paragraph A1-c for steady-ahead operation in a calm sea.

Using model experiments, the F_x, F_y, M_x, and M_y components can be calculated within $\pm$15 percent and the M_z component can be calculated within $\pm$30 percent.

Using statistical data, the F_x, F_y, M_x, and M_y components can be calculated within $\pm$25 percent, and the M_z component within $\pm$50 percent.

Transient and periodic loads. For given time-average ship speed and propeller rotational speed, the increase in transient and periodic loads** due to the influence of waves and ship motions can be estimated from existing experimental data. It is reasonable to disregard any transient variation in ship speed and propeller rotational speed (n). In practice, there is a small transient variation in V and n, the variation in n for a gas turbine propulsion system being dependent upon the propulsion control system.

NOTE:

* Time-average quantities are defined here as quantities averaged over a length of time that is much greater than the period of any significant component of the wave or ship motion of interest.

** Transient portion of quantities is defined here as the variation of time-average values per propeller revolution with local sea conditions and ship motions, and the periodic portion is defined as the variation with blade angular position.

The increase in transient loads is controlled primarily by the axial component of the orbital wave velocity at the propeller, and the increase in the periodic loads is controlled primarily by the vertical component of the orbital wave velocity at the propeller, as modified by the presence of the hull, and by the vertical velocity of the propeller due to ship motions.

For a given sea spectrum, the orbital wave velocities can be calculated directly from orbital wave theory. (Reference 11) Orbital wave velocities should be calculated at the depth of the propeller centerline.

The vertical velocity of the propeller due to ship motions depends upon the sea spectrum and the response of the hull in the pitch, heave, and roll modes. The response of the hull is best predicted by seakeeping experiments on a model of the hull. These experiments give information on the amplitudes and phases of the various components of hull response as functions of the lengths and orientations of the various wave components.

Determine the maximum transient loads in a rough sea $\bar{L}_{max,\zeta,\psi}$* as follows:

1. Calculate the minimum axial velocity at the shaft centerline from orbital wave theory for the assumed or specified sea spectrum, $V_A + V_{\zeta A,min}$ where V_A is the time-average axial velocity of advance derived form a thrust identity from the predicted powering performance in the rough sea and $V_{\zeta A,min}$ is the minimum axial velocity due to the waves ($V_{\zeta A,min}$ is negative so that $V_A + V_{\zeta A,min} < V_A$).
2. Calculate the maximum transient loads $\bar{L}_{max,\zeta,\psi}$ using loads estimated from open water theory and quasi-steady theory based on $V_A + V_{\zeta A,min}$ and the time-average n predicted in the rough sea.

Determine maximum periodic loads in a rough sea $\tilde{L}_{max,\zeta,\psi}$ as follows:

1. Calculate the periodic blade load $\tilde{L}$ that would occur if the ship were operating in a calm sea at the values of V and n that are predicted to occur in a rough sea. This may be estimated from the values calculated for steady-ahead operation in a calm sea, with adjustment for the differences in V and n between operation in a calm sea and in a rough sea, using the trends of existing data such as that in reference (6).
2. Calculate the maximum upward orbital wave velocity component V_ζ at the shaft centerline from orbital wave theory in the absence of the hull for the assumed or specified sea spectrum.

NOTE:

* The subscript ζ denotes the direct influence of the waves, and the subscript ψ denotes the influence of ship motions.

3. Calculate the maximum increase in periodic blade loads due to wave velocities from the corresponding loads that would occur if the ship were operating in calm water without ship motions at the same V and n as follows:

$$\Delta\tilde{L}_{\max,\zeta} = \frac{0.5\ V_\zeta}{V_c}\tilde{L}$$

where $\Delta\tilde{L}_{\max,\zeta}$ = maximum increase in periodic loads with waves over the values in calm water at the values of V and n that occur in a rough sea

$\tilde{L}$ = periodic blade loads in calm water at the values of V and n that occur in a rough sea

V_ζ = maximum vertical component of the orbital wave velocity in the propeller plane neglecting the influence of the hull

V_c = crossflow velocity component that would produce the estimated blade load L in calm water. For high speed transom sterns with exposed shafts and struts the crossflow velocity component is the first harmonic of the tangential wake at the 0.7 radius in calm water at the values of V and n that occur in a rough sea.

The 0.5 is an empirical factor applicable to ships with high speed transom sterns and exposed shafts and struts (see Reference 5) to account for the influence of the hull boundary in reducing the upward orbital velocity to below its calculated value in the absence of the hull. For other hull forms the effect of the hull may be approximated in a similar manner such as by deriving a different empirical factor. This factor or other suitable correction could be derived from model experiments similar to those described in Reference 5.

4. Calculate the maximum downward vertical velocity of the propeller from the pitch, heave, and roll modes of ship motions for operation in the assumed or specified sea spectrum.

5. Calculate the maximum increase in periodic blade loads due to ship motions from the corresponding loads that would occur if the ship were operating in calm water without ship motions at the same V and n as follows:

$$\Delta\tilde{L}_{\max,\psi} = \frac{0.6\ V_\psi}{V_c}\tilde{L}$$

where $\Delta\tilde{L}_{\max,\psi}$ = maximum increase in periodic loads with ship motions over the values in calm water without ship motions at the values of V and n that occur in a rough sea

$\tilde{L}$ = periodic blade loads in calm water without ship motions, at the values of V and n that occur in a rough sea

V_ψ = maximum vertical velocity of the propeller due to ship motions

V_c = crossflow velocity component that would produce the estimated blade load $\tilde{L}$ in calm water.

The 0.6 is an empirical factor applicable to ships with high speed transom sterns and exposed shafts and struts (see Reference 5) to account for the displacement effect of the hull above the propeller. This displacement effect induces a velocity at the propeller so that the velocity of the propeller relative to the local fluid particles is only 60 percent or less of the vertical velocity of the propeller. For other hull forms the effect of the hull may be approximated in a similar manner such as by using a different empirical factor. This empirical factor or other suitable correction could be derived from model experiments similar to those described in Reference 5.

6. Calculate the maximum periodic blade loads assuming that the increases in periodic loads due to wave velocities and due to ship motions occur simultaneously and, therefore, add in phase:

$$\tilde{L}_{max,\zeta,\psi} = \tilde{L} + \Delta\tilde{L}_{max,\zeta} + \Delta\tilde{L}_{max,\psi}$$

The assumption that these two increases add directly in phase is justified by previous research. Any error in this assumption is conservative.

The maximum value of the peak loads, including both transient and periodic contributions, may then be calculated assuming that the maximum values of the periodic loads and transient loads occur simultaneously and, therefore, add in phase as:

$$L_{peak,\zeta,\psi} = \bar{L}_{max,\zeta,\psi} + \tilde{L}_{max,\zeta,\psi}$$

The assumption that these two values add directly in phase is justified by previous research. Any error in this assumption is conservative.

If ship motions and time-average conditions and loads in a rough sea are predicted based on model experiments, and if loads under steady-ahead motion in a calm sea are predicted by the best available methods, then the maximum values of $\bar{F}_x$, $\bar{F}_y$, $\bar{M}_y$, and $\bar{M}_y$ due to operation in a rough sea can be predicted within approximately ± 20 percent. The maximum values of $\tilde{F}_x$, $\tilde{F}_y$, $\tilde{M}_x$, and $\tilde{M}_y$ can be predicted within ± 30 percent, and the maximum values of $\bar{F}_x + \tilde{F}_x$, $\bar{F}_y + \tilde{F}_y$, $\bar{M}_x + \tilde{M}_x$, and $\bar{M}_y + \tilde{M}_y$ can be predicted within ± 25 percent. The deviations from the true values for the M_z components are approximately twice the percentages for the other components. If ship motions or time-average conditions and loads in a rough sea are estimated from different hulls or propellers, the inaccuracies in predicting transient and periodic blade loads in a rough sea become somewhat greater.

APPENDIX 2

GUIDELINES FOR MINIMIZING BLADE LOADS

A2-a. Introduction

There are many variables that influence propeller blade loads. Blade loads can be reduced if the influences of these variables on propeller blade loads are considered in the design process.

Some guidelines for minimizing blade loads are consideration of the stern geometry, preliminary propeller design, detailed propeller blade design, the propulsion control system, and operating guidelines.

A2-b. Stern geometry

Several variables relating to the stern geometry of a high-speed transom stern configuration with exposed struts and shafting influence blade loads. However, these variables will be controlled by many criteria other than blade loads.

The general influences of the more important variables are as follows:

1. Number of propellers. For a given total delivered power and required thrust, increasing the number of propellers decreases the time-average loads per propeller. For all other parameters held constant, which is unrealistic, the number of propellers or time-average load per propeller does not have a first order influence on the periodic blade loads.
2. Inclination of the shaft. The periodic blade loads increase monotonically with the inclination of the shaft relative to the stern. The time-average loads are not sensitive to the shaft inclination. From consideration of periodic blade loads, the inclination of the shaft to the stern should be minimized. However, decreasing the shaft inclination may result in reduced tip clearances which may increase the propeller-induced periodic forces on the hull.

A2-c. Preliminary propeller design

Variables such as propeller diameter, pitch-diameter ratio, and number of blades may have a significant influence on blade loads. However, these variables will be controlled by many criteria other than blade load.

The general influences of the more important variables are as follows:

1. Diameter. Reducing the diameter reduces the moment arms to the hub and, thereby, reduces the bending moments.
2. Number of blades. Increasing the number of blades reduces the time-average and periodic loads per blade. However, this advantage tends to be offset by the reduced space per blade on and inside the hub.
3. Pitch-diameter ratio P/D (controlled by the rotational speed and diameter). Lower values of P/D tend to reduce the time-average transverse force per unit of thrust, and, thereby, reduce the time-average blade bending moments for a given thrust. Changing values of P/D

changes several factors such as rotational speed and blade pitch angle, which influence periodic blade loads in different ways; therefore, it is difficult to generalize on the influence of P/D on periodic blade loads.

A2-d. Detailed propeller blade design

Once the preliminary design of the propeller is completed, so that the propeller diameter, rotational speed, and number of blades are fixed, there is relatively little that the designer of the propeller can do to minimize blade loads, with the exception of the M component.

Specific recommendations are as follows:

1. Use balanced skew (skew forward at the inner radii and skew back at the outer radii) and no rake or forward rake (Reference 12).The forward skew at the inner radii, which is inherent in balanced skew, results in blade geometry near the blade-palm juncture that is more desirable for evenly distributing the loads among the blade attachment bolts than is zero or aft skew. Balanced skew is also desirable from consideration of bending moments due to centrifugal and gravitational forces and for minimizing time-average blade spindle torque. With proper selection of skew and rake, the net time-average spindle torque M arising from hydrodynamic and centrifugal loads can be made vanishingly small under steady-ahead operation in a calm sea. Skew also has advantages unrelated to blade loading, such as reduced propeller-induced unsteady hull forces, reduced blade frequency bearing forces and moments, and improved cavitation performance. However, practical amounts of skew do not measurably reduce the periodic hydrodynamic blade loads arising from the inclination of the flow.
2. Unload the blade tips. This moves the radial centers of the time-average hydrodynamic loads closer to the hub and, thereby, reduces the moment arms and moments in the hub. This may reduce the time-average moments by approximately eight percent relative to an optimum radial distribution of loading. Unloading the blade tips has other advantages unrelated to blade loading, such as reducing propeller-induced unsteady hull forces and suppressing tip vortex cavitation.

A2-e. Propulsion control system

The propulsion control system of a gas turbine powered ship has a dominant influence on the propeller blade loads during maneuvers, including acceleration, deceleration, and turning maneuvers. The propulsion control system controls the variation of the propeller rotational speed and pitch during a maneuver and may limit the maximum time-average torque per revolution to the propeller. Further, during turning maneuvers, the propulsion control system may control the different propellers of a multipropeller ship independently from one another.

A computer dynamic simulation of the complete propulsion system and ship response is an effective tool for establishing control system characteristics to obtain a good balance between values of peak propeller blade loads in maneuvers and ship maneuvering characteristics.

Therefore, the propulsion control system should be designed with the aid of computer dynamic simulations and the associated supporting model experiments to obtain the optimum balance between minimizing the values of peak propeller blade loads in maneuvers and superior ship maneuvering characteristics.

A2-f. Operating guidelines

In addition to the automated operating conditions during maneuvers, which are controlled by the propulsion control system as discussed in paragraph A2-e, there are manually controlled operating conditions which can have a large influence on propeller blade loads. One important example of this is voluntary speed reduction (power reduction) for operation in rough seas. The transient and periodic blade loads in rough seas vary approximately in proportion to the square of the propeller rotational speed. Guidance should be provided for manually controlled operating conditions that have a significant influence on propeller blade loads.

APPENDIX 3

COMPARISON METHOD FOR BLADE BOLTS AND CLOSED FORM STRESS ANALYSIS METHODS FOR BLADE BOLTS AND BLADE CARRIER

A3-a. Simple comparison method for blade bolts

In the simple comparison method, comparisons are made with blade bolt attachments which have had previous operating experience. Bolt forces are calculated based on several simplifying assumptions shown schematically in Figure 3.1. The moment due to the hydrodynamic force acting on the blade is assumed to be resisted by one bolt in tension on the pressure side of the blade. The bolt is also assumed to resist 25 percent of the centrifugal force regardless of the number of bolts. The applied forces and moments are balanced as indicated in Figure 3.1.

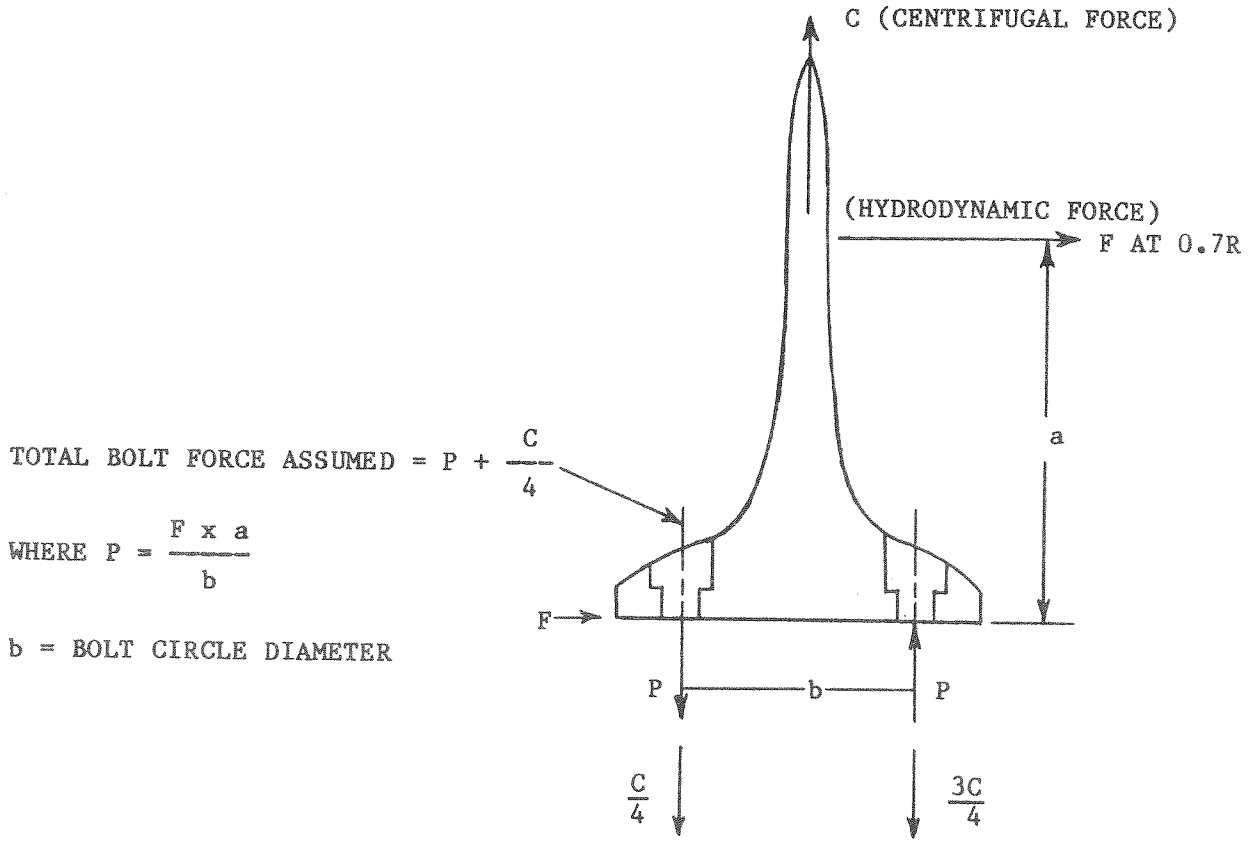

Figure 3.1 - Assumptions for Comparison Method for Blade Bolts

The hydrodynamic force is assumed to act at the 70 percent radius and is calculated based on design shaft horsepower and rotational velocity. The centrifugal force is computed based on the mass of the blade and blade palm, the rotational velocity, and the location of the blade center of gravity.

The bending moment caused by the hydrodynamic force F is assumed to be equivalent to a couple, F x a, where a is the distance between the underside of the blade in way of blade bolts and the 70 percent radius. This couple, F x a, is resisted by a similar couple, P x b, where P is the resisting force in the bolt and b is the bolt circle diameter.

With the above assumptions, a total bolt force can be computed which is an indication of the maximum possible bolt force at the design horsepower level Bolt stress associated with that force is then computed as force divided by shank area and compared with bolt prestress. Because the actual prestress obtained during assembly is generally only poorly known, the comparisons are based on the designer specified prestress, where it is available, or on a prestress equal to 40 percent of the yield stress of the bolt material which appears to be a typical design value. Comparisons of the ratios of bolt stress divided by bolt prestress based on the above method for more than 30 propellers show that if the ratio is greater than 1.0, potential bolt fatigue problems exist. It must be noted that the ratio could be greater than 2.0 for a satisfactory design if there is a good distribution of bolt forces.

A3-b. Closed form stress analysis methods for blade bolts

There are three strength criteria for use with the closed-form stress analysis methods for blade bolts. In equation form these are:

1. Maximum bolt shank stress ———— $S_{B,max} \leq 0.67 \times SY_B$ (1)

2. Maximum average stress under bolt head - $S_{BH,max} \leq 0.9 \times SY_{BL}$ (2)

3. Maximum fatigue stress ———— $S_{EFF,max} \leq 0.4 \times S_{END}$ (3)

where SY_B, SY_{BL} = 0.2 percent offset yield stress of bolt and blade materials, respectively
S_{END} = 0.4 x ultimate tensile strength of bolt material

The maximum bolt shank stress, $S_{B,max}$, for Equation (1) is calculated as follows regardless of the number of bolts:

$$S_{B,max} = S_{prestress} \times \left[1.0 + 2.0 \times 0.2 \times \left(\frac{F_{bolt,max}}{F_{preload}} \right)^{1.6} \right] \quad (4)$$

where $S_{prestress}$ = Average bolt prestress

$$F_{bolt,max} = \frac{C_{max}}{4} + \left[M_{max} \times \frac{(Y_{max} + r_{bolt})}{\sum_{all\ i} y_i^2} \right] \quad (5)$$

C_{max}, M_{max} = The centrifugal force and peak hydrodynamic bending moment (mean plus alternating) at the ship operating condition at which the maximum bolt stress will occur. Usually, this is during full-rudder, full-power turns, but the effect of rough seas during other operations should be considered.

0.2 and 1.6= Constants describing curve shown in Figure 3.2

2.0 = Constant for bolt bending due to applied loads

Y_{max} = Maximum distance of any bolt on the pressure side of the blade from the bolt center to the assumed neutral bending axis.

y_i = Distance from the center of any bolt i to the neutral bending axis assumed to intersect blade palm at its center

r_{bolt} = Bolt radius

$F_{preload}$ = bolt preload

The neutral bending axis is assumed to be parallel to the nose-tail line at the 0.7 radius and to intersect the blade palm at its center.

The maximum average stress under the bolt head, $S_{BH,max}$, for Equation (2) is calculated as follows:

$$S_{BH,max} = \frac{F_{bolt,max}}{A_{contact}} \tag{6}$$

where $A_{contact}$ = Area under the bolt head in contact with blade palm

The maximum fatigue stress, $S_{EFF,max}$, for Equation (3) is calculated as follows

$S_{EFF,max}$ = Maximum effective, fully-reversed alternating stress for full-rudder, full-power turn loading, corrected for effect of mean stress

for bolts with $SU_B < 100{,}000$ psi

$$S_{EFF}^{*} = \frac{k \times S_{B,alt}}{1 - \frac{(SY_B - k \times S_{B,alt})}{SU_B}} \tag{7}$$

for bolts with $SU_B \geq 100{,}000$ psi

$$S_{EFF}^{**} = \frac{7 \times k \times S_{B,alt}}{8 - \left[1 + \frac{(SY_B - k \times S_{B,alt})}{SU_B}\right]^3} \tag{8}$$

where k = Fatigue notch factor; 4 for cut threads, 3 for rolled threads

NOTE:

* Modified Goodman mean stress correction.

** Peterson mean stress correction.

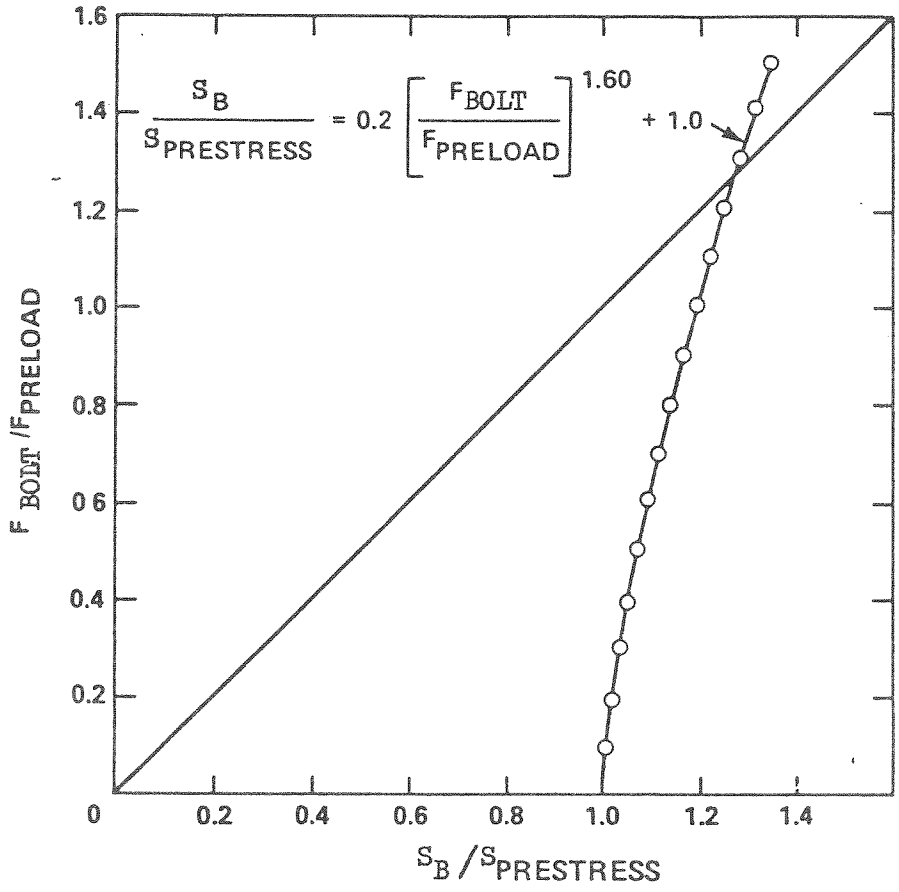

Figure 3.2 - Relationship between Joint Force and Average Tension Bolt Stress

$$S_{B,alt} = S_{prestress} \times 2.0 \times 0.2 \times \left[\left(\frac{F_{B,max}}{F_{preload}} \right)^{1.6} - \left(\frac{F_{B,min}}{F_{preload}} \right)^{1.6} \right] \quad (9)$$

$$F_{B,max} = \frac{C_{FPT}}{4} + \left[M_{FPT,max} \times \frac{(y_{max} + r_{bolt})}{\sum_{\text{all i}} y^2} \right] \quad (10)$$

$$F_{B,min} = \frac{C_{FPT}}{4} + \left[M_{FPT,min} \times \frac{(y_{max} + r_{bolt})}{\sum_{\text{all i}} y^2} \right] \quad (11)$$

$M_{FPT,min}$ = Difference of mean minus alternating bending moment in full-rudder, full-power turn due to hydrodynamic blade loads
$M_{FPT,max}$ = Sum of mean plus alternating bending moment in full-rudder, full-power turn, due to hydrodynamic blade loads
C_{FPT} = Centrifugal force of blade and bolts in full-power, full-rudder turn
SU_B = Ultimate tensile strength of bolt

A3-c. Closed Form Stress Analysis Methods for Blade Carrier

There are two strength criteria for use with the closed form stress analysis methods for the crank ring or trunnion type of blade carrier. In equation form, these are:

1. Maximum stress ———— $S_{BC,max} \leq 0.5 \times SY_{BC}$ (12)

2. Maximum fatigue stress - $S_{EFF,max} \leq 0.4 \times S_{END}$ (13)

where SY_{BC} = 0.2 percent offset yield stress of blade carrier material
S_{END} = 0.4 x ultimate tensile strength of blade carrier material
$S_{BC,max}$ = Maximum stress in the blade carrier as computed from Equation (14) or (26)
$S_{EFF,max}$ = Maximum effective, fully-reversed alternating stress for full-power, full-rudder turn loading, corrected for effect of mean stress, as computed from Equation (27).

The maximum stress for a crank ring, $S_{BC,max}$, for Equation (12) is calculated as follows:

$$S_{BC,max} = k_{BC} \times \left[S_{9,PC} + S_{9,PM} \times \frac{S_{13}}{S_{15}} \right] \quad (14)$$

where $S_{9,pc}$ and $S_{9,pm}$ = Nominal stress in crank ring fillet from Equation (15) pressures, P_c and P_m, in Figure 3.3 at the maximum loading as defined for Equation (5).

S_{13}, S_{15} = Stresses from Equations (16) and (17) at the maximum loading as defined for Equation (5).

k_{BC} = Stress concentration factor in crank ring fillet.

$$S_9 = \frac{6 \times P \times R_o^2}{t^2 \times C_8} \times \left[\frac{C_9}{2 \times R_o \times R_i} \times (R_o^2 - R_b^2) - L_{17} \right] \quad (15)$$

$$S_{13} = \frac{B \times M_{max}}{(R_o \times t^2)} \quad (16)$$

$$S_{15} = \frac{A \times R_o \times M_{max}}{I} \times \frac{3}{\pi \times t^2} \times \frac{R_o}{R_i} \times \frac{C_9}{C_8} \quad (17)$$

where P = P_c or P_m from Figure 3.3

$P_c = \frac{C_{max}}{A}$ = uniform pressure

$P_m = \frac{R_o \times M_{max}}{I}$

M_{max} = Peak hydrodynamic bending moment at maximum loading condition (same as for Equation (5))

C_{max} = Applied centrifugal force at maximum loading (same as for Equation (5))

A = Area of bearing surface = $\pi \times (R_o^2 - R_b^2)$

t = Flange thickness, Figure 3.3

R = Radius of thick portion of crank ring, Figure 3.3

R_o = Outer radius of flange of crank ring, Figure 3.3

R_b = Inner radius of bearing surface under pressure, Figure 3.3

$$C_8 = \frac{1}{2} \times \left\{ 1 + \nu + \left[(1 - \nu) \times \left(\frac{R_i}{Ro} \right)^2 \right] \right\} \quad (18)$$

$$C_9 = \frac{R_i}{R_o} \times \left\{ \frac{1 + \nu}{2} \times \ln\left(\frac{R_o}{R_i} \right) + \frac{1 - \nu}{4} \times \left[1 - \left(\frac{R_i}{R_o} \right)^2 \right] \right\} \quad (19)$$

$$L_{17} = \frac{1}{4} \times \left\{ 1 - \frac{1-\nu}{4} \times \left[1 - \left(\frac{R_b}{R_o} \right)^4 \right] - \left(\frac{R_b}{R_o} \right)^2 \times \left[1 + (1+\nu) \times \ln\left(\frac{R_o}{R_b} \right) \right] \right\} \quad (20)$$

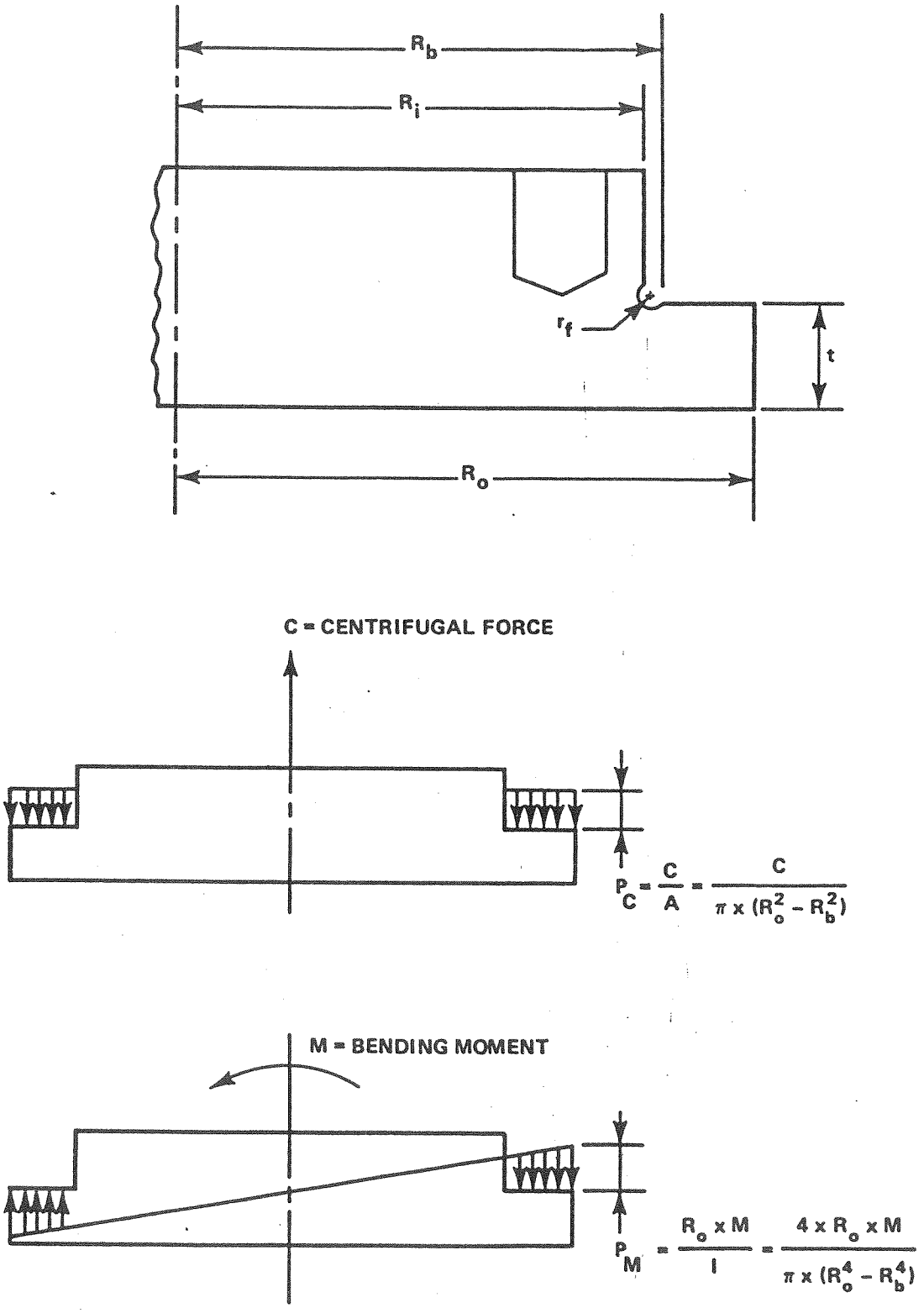

Figure 3.3 - Crank Ring Dimensions and Terminology

where ν = Poisson's Ratio

$$B = 2.9375\ g^2 - 7.315g + 4.412125 \quad (21)$$

$$g = \frac{R_i}{R_o} \quad (22)$$

$$I = \frac{\pi}{4} \times (R_o^4 - R_b^4) \quad (23)$$

Use of Equations (15), (16), and (17) to predict crank ring fillet stresses should be limited to geometries in which the minimum distance between blade bolt threads and crank ring fillet is large enough to keep the effect of thread loading on fillet stress to an insignificant level. A crude method for estimating this limiting distance is:

$$(t_{wall})_{limit} \geq 6.0 \times 10^{-3} \times \text{bolt force} \quad (24)$$

where $(t_{wall})_{limit}$ = limiting distance between bolt threads and fillet

$$\text{bolt force} = F \times \frac{a}{b} + \frac{c}{4} \quad \text{(See Figure 3.1)} \quad (25)$$

F = Hydrodynamic force at design condition
a = Distance between underside of blade palm at crank ring bolting face and 70 percent blade radius
b = Blade bolt circle diameter
C = Centrifugal force at design condition

The maximum stress for a trunnion, $S_{BC,max}$, at the cross section giving the highest stress, for Equation (12) is calculated as follows:

$$S_{BC,max} = k_{bc} \times \left[\left(\frac{C_{max}}{A}\right) + \left(\frac{M_{max}}{Z}\right)\right] \quad (26)$$

where k_{bc} = Stress concentration factor in trunnion fillet.
C_{max} and M_{max} as defined in Equation (5)
A = Area of cross section
Z = section modulus of cross section

The maximum effective, fully-reversed alternating stress for either the crank ring or the trunnion for Equation (13), $S_{EFF,max}$, is found with the modified Goodman mean stress correction as follows:

$$S_{EFF,max} = \frac{S_{BC,alt}}{1 - \frac{S_{BC,mean}}{SU_{BC}}} \quad (27)$$

where $S_{BC,alt}$ and $S_{BC,mean}$ are obtained using Equation (14) or Equation (26) with the appropriate values for centrifugal force, C, and bending moment, M, at the full power turn operating condition. These are C_{FPT} for centrifugal force (same as for Equations (10) and (11)), and $M_{FPT,alt}$ and $M_{FPT,mean}$ for bending moments

$M_{FPT,mean} = (M_{FPT,max} + M_{FPT,min}) \times 0.5$

$M_{FPT,alt} = M_{FPT,max} - M_{FPT,mean}$

SU_{BC} = Ultimate tensile strength of the blade carrier material.